

広島大学学術情報リポジトリ
Hiroshima University Institutional Repository

Title	Highly sensitive ion detection using Si single-electron transistors
Author(s)	Kudo, Takashi; Nakajima, Anri
Citation	Applied Physics Letters , 98 (12) : 123705
Issue Date	2011
DOI	10.1063/1.3569148
Self DOI	
URL	http://ir.lib.hiroshima-u.ac.jp/00034090
Right	(c) 2011 American Institute of Physics
Relation	



Highly sensitive ion detection using Si single-electron transistors

Takashi Kudo and Anri Nakajima^{a)}

Research Institute for Nanodevice and Bio Systems, Hiroshima University, 1-4-2 Kagamiyama, Higashihiroshima, 739-8527, Japan

(Received 24 December 2010; accepted 1 March 2011; published online 24 March 2011)

Si single-electron transistors (SETs) were used for highly sensitive ion detection. A multiple-island channel structure was adapted in the SET for room-temperature operation. Clear Coulomb oscillation and diamonds were observed at room temperature. Using the Coulomb oscillation, clear pH responses of drain current (I_d)-gate voltage (V_g) characteristics were obtained despite the existence of I_d noise. Because Coulomb oscillations have a possibility to increase the slope of I_d over V_g near the half-maximum current of the peaks, high resolving power of ion, and/or biomolecule concentration can be expected. A Si-structure will make it possible to integrate the sensors on a single chip. © 2011 American Institute of Physics. [doi:10.1063/1.3569148]

The detection and quantification of chemical and biological species are central to many areas of healthcare and the life sciences, ranging from the diagnosis of disease to the discovery of new drug molecules. Field effect transistors (FETs) are sophisticated devices used for the detection of charged molecules.¹ Ion-sensitive FETs change their electrical characteristics in response to the concentration and type of ions present in aqueous solutions on the gate insulator surface. Furthermore, biosensors, and biochips based on FETs have recently been developed for the detection of DNA, proteins, and viruses.²⁻⁹ These methods are used to measure changes in charge accompanied by specific molecular recognition events on the gate insulator surface of FETs. High sensitivity in detecting target ions or biomolecules has been obtained using nanowire channels in FET sensors.⁹⁻¹¹ However, FET sensors with even higher sensitivity in detecting targets are preferable, especially in dilute solutions of targets, where large noise exists in the drain current (I_d)-gate voltage (V_g) characteristics. Therefore, we have proposed a FET sensor utilizing a single-electron transistor (SET) for highly sensitive ion and/or biomolecule detection. High resolving power of ions and/or biomolecule concentration can be expected using Coulomb oscillation. Since room-temperature operation is necessary for ion and/or biomolecule sensing, a multiple-island system is effective for SETs. Moreover, a Si-structure is important since we can use existing large scale integration (LSI) technology in the fabrication, and the fabricated FET sensors can be integrated on a single chip for simultaneous detection and quantification of various ions and/or biomolecules. Therefore, in this study, we fabricated a Si SET sensor with multiple islands for highly sensitive pH detection (one type of ion detection) and demonstrated its fundamental electrical characteristics.

We fabricated a one-dimensional array of nanoscale islands in a silicon-on-insulator (SOI) layer by using electron beam lithography. There were 11 islands, and the channel length was 3 μm . We used a p-type (B doped) SOI (100) wafer (13.5–22.5 $\Omega\text{ cm}$). No channel doping was performed. The device fabrication process is as follows. After the etching of the island array with an electron cyclotron resonance

etcher using the resist pattern as a mask, subsequent isotropic wet etching in an $\text{NH}_4\text{OH}/\text{H}_2\text{O}_2/\text{H}_2\text{O}$ solution¹² was carried out to reduce the dimensions of the array [Fig. 1(a)]. Next, the oxidation was carried out to further reduce the size of the islands and the width of the wire regions, which act as tunnel barriers for electrons. The final island size and wire width was about 50 nm and 30 nm, respectively. The final thickness of the top-Si was about 18 nm. After the source and drain areas were formed by ion implantation of As^+ at 30 keV with a dose of $4 \times 10^{15}\text{ cm}^{-2}$, we fabricated $\text{Si}_3\text{N}_4/\text{SiO}_2$ stacked gate insulators as follows. A layer of SiO_2 about 9 nm thick was thermally grown at 850 $^\circ\text{C}$ in a dry atmosphere followed by the deposition of about 36 nm thick Si_3N_4 by low-pressure chemical vapor deposition at 750 $^\circ\text{C}$.

A schematic diagram of our measurement system is shown in Fig. 1(b). A fluidic channel was made of polydimethylsiloxane (PDMS). The volume of the cell was as follows: the size of the fluidic channel on the FET was approximately 3 mm \times 1 mm \times 100 μm (length \times width \times height). The entire area of the SET including the Al pad electrodes

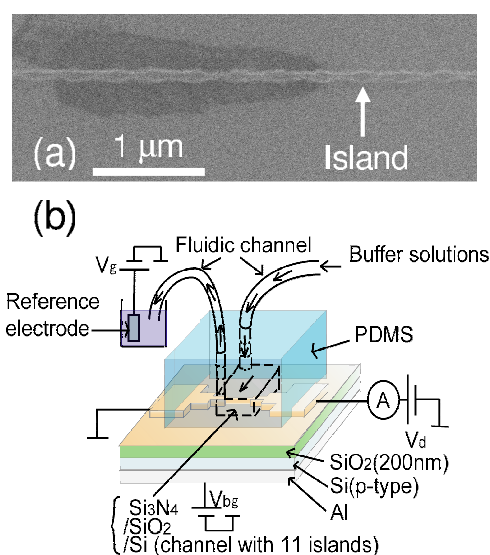


FIG. 1. (Color online) (a) Scanning electron micrograph (SEM) of the channel region of the fabricated Si SET with 11 islands after dry and wet etching. The dark area is due to a long time high resolution SEM observation. (b) Schematic diagram of measurement system.

^{a)} Author to whom correspondence should be addressed. Electronic mail: anakajima@hiroshima-u.ac.jp.

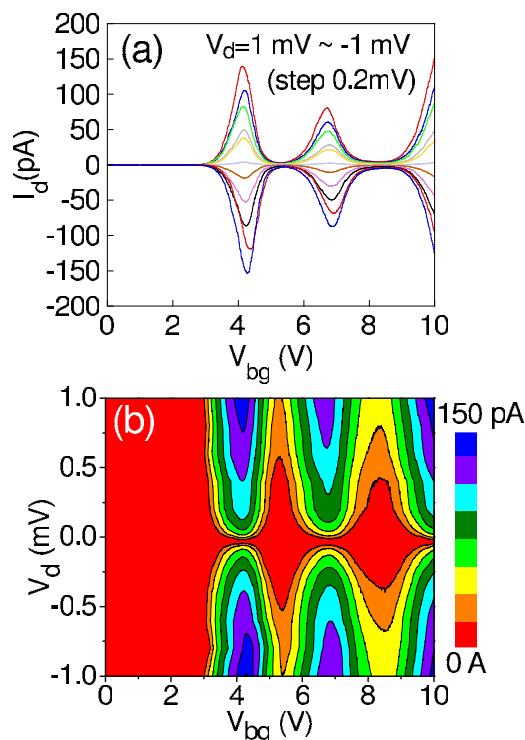


FIG. 2. (Color online) (a) Drain current (I_d) vs back-gate voltage (V_{bg}) characteristics as a function of drain-source voltage (V_d) at room temperature for the fabricated SET with 11 islands. V_d from -1 to 1 mV in V_d steps of 0.2 mV. (b) Contour plot of I_d as a function of V_d and V_{bg} at room temperature. Devices with larger dot size and barrier width did not show Coulomb oscillations.

(0.25 mm^2) was 1.2 cm^2 . The joining surface of the PDMS was modified by O_2 plasma treatment and then attached to the SET. An Ag/AgCl reference electrode was used to control the V_g of the SET through a buffer solution. The electrical characteristics were measured using a semiconductor parameter analyzer (B1500A, Agilent).

First, we investigated the electrical characteristics of the fabricated SET under the absence of buffer solutions on the $\text{Si}_3\text{N}_4/\text{SiO}_2$ stacked gate insulators. In this measurement, the gate voltage was applied through the backside of the device (Si substrate of the SOI wafer). Figure 2(a) plots I_d versus back-gate voltage (V_{bg}) characteristics at room temperature. The drain-source voltage (V_d) was varied from -1 to 1 mV in V_d steps of 0.2 mV. Two peaks of Coulomb oscillation were confirmed around $V_{bg} = 4$ and 7 V. Figure 2(b) shows the contour plot of I_d as a function of V_d and V_{bg} evaluated from Fig. 2(a). Clear Coulomb diamonds were observed. The positions of the two peaks of Coulomb oscillation in Fig. 2(a) correspond to the constricted parts in Fig. 2(b). Therefore, room-temperature SET operation was confirmed for the fabricated devices. The high temperature operation is thought to have been achieved due to a serially connected multiple-island system as discussed later.

Figure 3 plots the I_d versus V_g characteristics at a V_d of 1 mV for three different buffer solutions: 50 mM phthalate, $\text{pH } 4$; 50 mM phosphate, $\text{pH } 7$; and 10 mM tetraborate, $\text{pH } 9$. In this measurement, the reference electrode in the buffer solutions was used as a gate while keeping $V_{bg} = 0$ V. We confirmed a linear relationship between the solution potential and V_g ($0 < V_g < 2$ V) with a slope close to one, indicating no electrochemical reactions took place in

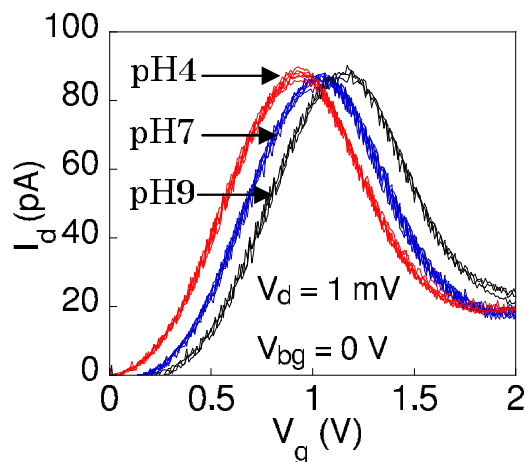


FIG. 3. (Color online) Drain current (I_d) vs gate voltage (V_g) characteristics of the SET with 11 islands for three different pH values at room temperature. The drain-source voltage (V_d) was fixed at 1 mV. The back-gate voltage (V_{bg}) was also fixed at 0 V. The leakage current between the reference electrode and source/drain contact is very small and keeping the value within 2 pA less than the noise level at the V_g range from 0 to 2 V, ensuring the measurement reliability.

solution at the V_g range. The flow rate of the solutions was $0.1 \mu\text{l}/\text{min}$. The buffer solution was changed from $\text{pH } 4 \rightarrow 7 \rightarrow 9 \rightarrow 7 \rightarrow 4$ to confirm the reproducibility of the pH response. For every pH change, I_d - V_g measurements were carried out three times to investigate the stability under a constant pH. Both in the increase in pH ($\text{pH } 4 \rightarrow 7 \rightarrow 9$) and the decrease in pH ($\text{pH } 9 \rightarrow 7 \rightarrow 4$), the I_d - V_g curves for the same pH coincide well. The small hysteresis (threshold voltage shift less than 5 mV) insures the high resolution pH detection. As can be seen in the figure, a clear Coulomb oscillation peak was observed for each pH value. The peak position varied with the pH of the buffer solution. For $V_g > 2$ V, we did not carry out measurements due to the large leakage currents between the reference electrode and back-gate (typically about 3 nA at $V_g = 2$ V). Because there was no peak in Coulomb oscillation for $V_g < 0$ V in Fig. 3, this peak is assumed to correspond to the first peak of Coulomb oscillation (around 4 V of V_{bg}) in Fig. 2(a).

A summary of the pH response characteristics of the SET is plotted in Fig. 4. Because there is some noise in the measured I_d - V_g curves in Fig. 3, each measured I_d - V_g curve of Coulomb oscillation was fitted using a least-squares pro-

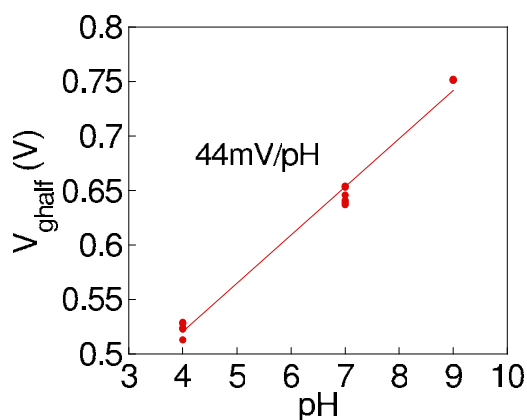


FIG. 4. (Color online) pH response characteristics of the fabricated SET with 11 islands at room temperature.

gram, and the V_g values were obtained at the left side half-maximum current of each fitted curve in order to precisely evaluate the pH sensitivity. The obtained V_g value ($V_{g, \text{half}}$) was shifted in the positive (negative) direction as the pH of the buffer solution was increased (decreased). The slope of the calibration curve ($V_{g, \text{half}}$ versus pH curve) is about 44 mV/ pH , which agrees well with previous experimental results (46–56 mV/ pH).¹³ The slight difference in our experimentally obtained value and the theoretical value (58 mV/ pH , 20 °C) may be due to the oxygen content in the Si_3N_4 layer.¹³ These results show that reproducible pH responses were obtained with the fabricated SET.

The possible advantage of using SETs as ion and/or biomolecule sensors is as follows. In an SET, Coulomb oscillations with a symmetry shape and the same peak height appear when the barrier conductance is constant in the whole V_g regions according to the orthodox theory.¹⁴ However, when the dependence of barrier conductance on V_g exists, Coulomb oscillations are modulated and weighted by the variation in the barrier conductance. Therefore, if the barrier conductance increases with V_g , it is possible that the final slope of I_d over V_g in the SET becomes larger than that of the barrier itself. Especially in SETs with barriers consisted of semiconductor nanowires with low doping level, this situation can occur and the slope can be larger than that of the nanowire itself. In such a case, the largest slope can be obtained around a V_g near the left side half-maximum current of the peaks in SETs. Under conditions where large I_d noise exists, the larger slope of I_d over V_g leads to a better resolving power of ion and/or biomolecule concentration. Also, there is an advantage of utilizing SETs to evaluate the target concentration value from only the change in I_d at $V_g=0$ V. In this case, there is a merit that it is not necessary to sweep V_g for searching a threshold voltage (V_{th}). For that purpose, conventional metal-oxide-semiconductor field-effect transistors with highly doped channel were generally used in accumulation to measure the I_d change at a fixed V_g of 0 V for the pH detection. However, in accumulation highly doped channel shows the metal like conduction: the slope of I_d over V_g is small. Accordingly, it is difficult for V_{th} change with a small pH change to be detected if relatively large I_d noise exists, leading to the difficulty in high resolution pH detection. Instead, if we use an SET pH sensor with highly doped channel region including Coulomb islands and barriers, high resolution pH detection becomes possible due to the Coulomb oscillation: the slope of I_d over V_g becomes larger. This leads to the merit of high resolution pH detection without sweeping V_g .

For ion and/or biomolecule sensing, room-temperature operation is strongly required. To achieve room-temperature operation of an SET with a single island, the island, and junction sizes should be reduced to less than 10 nm in order to reduce the total capacitance.¹⁵ However, it is difficult to fabricate such structures reproducibly by using currently available LSI fabrication techniques. One way to overcome the difficulty is to utilize serially connected islands instead of a single island. In such a multiple-island system, the effective total capacitance of each island decreases compared with that in a single-island system because the junction capaci-

ties are connected in series.^{15,16} This leads to an increase in the charging energy of each island and to an increase in the operation temperature. In other words, to enable room-temperature operation, a multiple-island system can use a larger island than that used by a single-island system. Moreover, SETs with serially connected islands can suppress cotunneling,¹⁷ which increases the valley current of Coulomb oscillation and prevents higher temperature operation.¹⁸ To date, we have applied an SET with multiple islands connected in series to an exclusive-OR (XOR) circuit, which achieved room-temperature operation.¹⁹ Therefore, we used the multiple-island system to realize room-temperature operation of an SET for highly sensitive pH sensing in this study. In fact, we were not able to obtain Coulomb oscillations at room-temperature in SETs with a single-island system in this study.

In summary, we fabricated a Si SET with multiple islands for pH sensors integrated on a single chip. Clear Coulomb oscillations and Coulomb diamonds were confirmed at room temperature. Clear pH responses of I_d - V_g characteristics were obtained by using Coulomb oscillations despite the existence of I_d noise. The slope of the calibration curve was 44 mV/ pH . Because Coulomb oscillations have a possibility to increase the slope of I_d over V_g near the half-maximum current of the peaks, a Si SET sensor with multiple islands is promising for future high sensitivity ion and/or biomolecule sensors integrated on a single chip.

¹P. Bergveld, *IEEE Trans. Biomed. Eng.* **19**, 342 (1972).

²F. Patolsky, G. Zheng, O. Hayden, M. Lakadamyali, X. Zhuang, and C. M. Lieber, *Proc. Natl. Acad. Sci. U.S.A.* **101**, 14017 (2004).

³W. U. Wang, C. Chen, K. Lin, Y. Fang, and C. M. Lieber, *Proc. Natl. Acad. Sci. U.S.A.* **102**, 3208 (2005).

⁴K. Park, M. Kim, and S. Choi, *Biosens. Bioelectron.* **20**, 2111 (2005).

⁵E. Stern, J. F. Klemic, D. A. Routenberg, P. N. Wyrembak, D. B. Turner-Evans, A. D. Hamilton, D. A. LaVan, T. M. Fahmy, and M. A. Reed, *Nature (London)* **445**, 519 (2007).

⁶M. Gotoh, E. Tamiya, I. Karube, and Y. Kagawa, *Anal. Chim. Acta* **187**, 287 (1986).

⁷T. Sakata, M. Kamahori, and Y. Miyahara, *Jpn. J. Appl. Phys., Part 1* **44**, 2854 (2005).

⁸T. Kudo, T. Kasama, T. Ikeda, Y. Hata, S. Tokonami, S. Yokoyama, T. Kikkawa, H. Sunami, T. Ishikawa, M. Suzuki, K. Okuyama, T. Tabei, K. Ohkura, Y. Kayaba, Y. Tanushi, Y. Amemiya, Y. Cho, T. Monzen, Y. Murakami, A. Kuroda, and A. Nakajima, *Jpn. J. Appl. Phys.* **48**, 06FJ04 (2009).

⁹G. Zheng, F. Patolsky, Y. Cui, W. U. Wang, and C. M. Lieber, *Nat. Biotechnol.* **23**, 1294 (2005).

¹⁰Y. Cui, Q. Wei, H. Park, and C. Lieber, *Science* **293**, 1289 (2001).

¹¹O. Knopfmacher, A. Tarasov, W. Fu, M. Wipf, B. Niesen, M. Calame, and C. Schonenberger, *Nano Lett.* **10**, 2268 (2010).

¹²A. Nakajima, H. Aoyama, and K. Kawamura, *Jpn. J. Appl. Phys., Part 2* **33**, L1796 (1994).

¹³H. Abe, M. Esashi, and T. Matsuo, *IEEE Trans. Electron Devices* **26**, 1939 (1979).

¹⁴K. K. Likharev, *Proc. IEEE* **87**, 606 (1999).

¹⁵K. Ohkura, T. Kitade, and A. Nakajima, *J. Appl. Phys.* **98**, 124503 (2005).

¹⁶A. Nakajima, Y. Ito, and S. Yokoyama, *Appl. Phys. Lett.* **81**, 733 (2002).

¹⁷K. Ohkura, T. Kitade, and A. Nakajima, *Appl. Phys. Lett.* **89**, 183520 (2006).

¹⁸Y. Takahashi, S. Horiguchi, A. Fujiwara, and K. Murase, *Physica B* **227**, 105 (1996).

¹⁹T. Kitade, K. Ohkura, and A. Nakajima, *Appl. Phys. Lett.* **86**, 123118 (2005).